Multi-parameter mapping of the human cervical spinal cord in brachial plexus root implantation

Rebecca Sara Samson[1], Carolina Kachramanoglou[1], David Choi[2], Antoine Lutti[3], David L Thomas[4], Nikolaus Weiskopf[3], Olga Ciccarelli[5,6], and Claudia A M Wheeler-Kingshott[1]

[1]NMR Research Unit, Department of Neuroinflammation, Queen Square MS Centre, UCL Institute of Neurology, London, England, United Kingdom, [2]Spinal Repair Unit, UCL Institute of Neurology, London, England, United Kingdom, [3]Wellcome Trust Centre for Neuroimaging, UCL Institute of Neurology, London, England, United Kingdom, [4]5Neuroradiological Academic Unit, Department of Brain Repair and Rehabilitation, UCL Institute of Neurology, London, England, United Kingdom, [5]NMR Research Unit, Department of Brain Repair and Rehabilitation, Queen Square MS Centre, UCL Institute of Neurology, London, England, United Kingdom, [6]6NIHR UCL/UCLH Biomedical Research Centre (BRC), London, England, United Kingdom

Target audience: Clinicians and scientists interested in measures of cord abnormalities following spinal cord injury and advanced spinal cord imaging.

Purpose: To investigate changes in the upper cervical cord following brachial plexus avulsion using multi-parameter mapping.

Introduction: Brachial plexus avulsion (BPA) injury may lead to paralysis and anaesthesia of the corresponding limb. Re-implantation of avulsed ventral roots is an effective surgical technique that leads to improved motor recovery (1). Structural MRI is insensitive to BPA, therefore newer quantitative MRI methods are required to investigate tissue microstructural changes following BPA, and may provide more sensitive non-invasive markers for therapy monitoring. We have developed a technique using multi-echo 3D FLASH to quantify several parameters in the brain (2,3,4) and spinal cord (5) including apparent proton density (APD), T_1, R_2^* (=1/T_2^*), MTR and a new parameter MT . We aimed to assess whether this quantitative multi-parameter mapping method detects pathological changes in the upper cervical cord (i.e. above the site of injury, which appears normal on conventional MRI) in patients with BPA who have received re-implantation, when compared with healthy subjects. In patients, the relationship between these new quantitative parameters and clinical outcome measures was explored.

Methods: ***Subjects:*** 8 BPA patients (all M, aged 32.8 yrs. ±9.7) treated with re-implantation, and 13 healthy controls (HC) (12M, 1F, aged 36.4±12.3) were included in this study. In each patient the complete avulsion injury was confirmed by direct visualisation of the brachial plexus and re-implantation was performed within 1 month of injury. Patient disability was assessed using the following scales: (i) Disability for Arm, Shoulder and Hand (DASH) questionnaire, (ii) Visual Analogue Pain Scale (VAS) self-assessment of pain, (iii) Medical Research Council (MRC) muscle strength assessment of 7 muscle groups for the upper limb.

MRI acquisition: All subjects were scanned on a 3T Magnetom TIM Trio scanner (Siemens Healthcare, Erlangen, Germany) with a head, neck and spine receiver array coil. 80 3mm thick partitions were acquired, with axial field-of-view (FOV)=200mmx200mm, 256x256 acquisition matrix, sinc interpolated in image space to 512x512, and phase encoding (PE) anterior/posterior, with GRAPPA acceleration factor 2 in the PE direction. A slab selective 3D multi-echo FLASH sequence (3,4) was performed 3 times, with PD (PDw; TR=24.05ms, flip angle (α)=6º), MT (MTw; with a 4ms off-resonance Gaussian RF pulse (nominal α=220º, offset frequency 2kHz) before each excitation pulse) or T_1 (T_1w; TR=22ms, α=20º) weighting. For the PDw images, magnitude and phase images were acquired from 8 bipolar gradient echoes at equally spaced echo times between 3.0ms and 18.55ms (425Hz/pixel BW) to enable calculation of R_2^*. The spatial distribution of the B_1 transmit field was measured using a modified 3D actual flip angle imaging (AFI) method (6) with alternative RF/gradient spoiling scheme (7), with two excitation pulses of α =60° followed by delays of 50 and 150ms and a gradient echo readout at TE=3.05ms. For the AFI acquisition, 40 6mm partitions were acquired, with FOV=200mmx200mm, and acquisition matrix 64x64, sinc interpolated to 512x512, to enable correction of the T_1 maps. The total scan time was 19 mins.

Image Analysis: Cord levels C1-C3 were extracted using FSL (http://www.fmrib.ox.ac.uk/fsl), then co-registration of images to a registration target generated from the averaged PDw, MTw and T1w images was performed as described in reference (5), using the FSL tool FLIRT, with degrees of freedom (DOF) = 6, cost function = normalised mutual information (the most suitable cost function for images of different contrast (8)), and sinc interpolation (5). B_1 data were also co-registered to the (registered) averaged T_1w data using 6DOF and cost function = mutual information, to enable correction of T_1 maps.

Processing routines developed for use with SPM8 and FSL were used for analysis (2,3,4). T_2^* was estimated from the multi-echo 'PDw' acquisition sequence, by linear fitting of the log of the signal. For the calculation of the other parameter maps, the first 6 echoes were averaged, and then T_1 and the amplitude APD (apparent PD) were calculated from the PDw and T_1w images via a rational approximation of the FLASH signal (3). The parameter MT represents the additional percentage MT saturation of the longitudinal magnetization due to a single MT pulse, and is calculated by inserting the estimated APD and T_1 values in the approximate signal equation for the MT-FLASH experiment (4).

Semi-automatic cord segmentation was performed on the T_1w images using a method based on an active surface model (9) (Jim www.xinapse.com). Masks were generated for each subject over 5 slices centred on cord level C2. The grey matter (GM) was outlined and regions of interest (ROIs) were drawn manually (on the averaged MTw image since this had the best white matter (WM)-GM contrast) using Jim 6.0 in the left (L) and right (R) lateral WM, and all ROI masks were applied to the parameter maps. Mean cord, GM and WM ROI parameter values ipsilateral (IL) and contralateral (CL) to the injured side were compared between patients and HC (with IL/CL compared to HC L/R average lateral WM values). All statistical analysis was performed using SPSS version 21.0 (SPSS, Inc., Chicago, IL, USA). Differences between BPA patient and HC parameter values were tested using Mann-Whitney U tests, and Spearman's Rho tests were used for correlations, since the data were not normally distributed.

Table 1: Mean parameter values (±SD) for all subjects (*=p<0.05; **=p<0.01 compared to HC)

C2 cord region	APD (a. u.)	MT (pu)	MTR (pu)	R_2^* (s^{-1})	T_1 (ms)
HC whole cord	4732(±736)	1.27(±0.13)	41.3(±2.13)	21.3(±1.80)	1823(±144)
BPA whole cord	4473(±761)	1.20(±0.057)	39.7(±1.99)	22.4(±3.43)	**1638(±208)***
HC L/R ave WM	4541(±729)	1.45(±0.15)	44.0(±1.94)	20.8(±1.86)	1625(±136)
IL WM	4208(±782)	1.39(±0.10)	42.5(±1.88)	**23.9(±4.48)***	1407(±252)
CL WM	4273(±858)	1.40(±0.17)	41.8(±4.71)	21.8(±3.92)	1444(±268)
HC GM	4908(±729)	1.21(±0.12)	40.9(±2.31)	19.4(±1.83)	1761(±110)
BPA GM	4654(±778)	**1.09(±0.074)****	**38.6(±1.01)****	20.0(±3.83)	1617(±214)

Results: Patients showed significantly reduced whole cord T_1, increased ipsilateral WM R_2^*, and reduced GM MT and MTR when compared with HC (see Table 1 values in bold). Example MTw, APD, T_1, MT, MTR and R_2^* maps for a single HC and BPA patient at C2 are shown in Figure 1.

Correlations with clinical scores: In patients, significant correlations between a greater abnormality in the MRI parameters and worse physical disability, as reflected by higher MRC scores, were found. In particular: whole cord: R_2^* (r=0.73, p<0.05), T_1 (r=-0.77, p<0.05); IL WM: APD (r=-0.76, p<0.05), R_2^* (r=0.92, p=0.001), T_1 (r=-0.85, p<0.01); GM: APD (r=-0.83, p<0.05), MT (r=0.73, p<0.05), R_2^* (r=0.83, p<0.05), T_1 (r=-0.83, p<0.05). No significant correlations between either VAS or DASH scores were found in any of the parameters.

Discussion: The technique described here is rapid and provides several quantitative MRI measures that may be sensitive to changes in the cervical cord following BPA and re-implantation. Over the whole cord at C2 level, T_1 was reduced in BPA patients compared to HC (p<0.05), which could be partly due to alterations in the GM/WM volume ratio in the cord (this was reduced from 0.173 in HC to 0.125 in BPA (p<0.001), but is probably not enough to fully explain the size of whole cord T_1 reduction observed here. It is also possible that there was an increase in the number of unmyelinated axons, as has been observed in animal models of nerve root avulsion injury (10) (non-significant T_1 reductions are also observed in WM and GM ROIs separately). In the WM region drawn on the IL side of cord most injured, R_2^* was increased compared to the HC L/R average value (p<0.05) (i.e. T_2^* was reduced), which may be related to axonal sprouting. MT and MTR were both reduced in the GM in BPA patients (p<0.01), which could be due to demyelination and/or axonal damage. Trends towards reductions in APD, MT, MTR, T_2^*, and T_1 can be seen in BPA compared to HC in all regions, but did not reach significance, probably due to the small number of subjects studied here (within-group variation was large).

The correlations between the MRI parameters and the MRC scores, which were stronger in the IL WM, suggest that the quantitative parameters measured here reflect underlying pathological changes that are responsible for clinical disability.

Our findings suggest that multi-parameter mapping of the upper cervical cord distal to the site of injury may provide insights into the underlying pathological changes in BPA patients following re-implantation. Future studies including larger numbers of patients and also including patients with BPA who did not undergo re-implantation are required, to provide further understanding of tissue structural changes that are specific to re-implantation.

References: [1] Carlstedt, TP. Microsurgery. 16(1):13-6 (1995),[2] Weiskopf N & Helms G Proc ISMRM 16: 2241 (2008), [3] Helms G *et al* MRM 59:667-72 (2008), [4] Helms G *et al.* MRM 60: 1396-1407 (2008), [5] Samson RS *et al.* NMR Biomed 26(12):1823-30 (2013), [6] Yarnykh V *et al.* MRM 57 (1): 192-200 (2000), [7] Lutti A *et al.* MRM 64: 229-38 (2010), [8] Maes F *et al* .IEEE Trans. Med. Imaging; 16(2): 187–198 (1997), [9] Horsfield MA et al NeuroImage 50 446-455 (2010), [10] Risling M *et al*. Exp Neurol. 83(1):84-97 (1984)

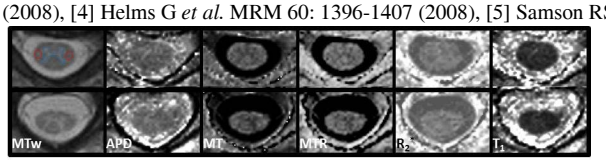

Figure 1: Example MTw (with WM (red) and GM (blue) APD, T_1, MT, MTR and R_2^* maps (L to R) for a HC (top) & BPA (bottom)

Acknowledgements: *This study was funded by the UCLH/UCL Biomedical Research Centre. RS is funded by the MS Society of the UK. .The scanning was performed at the the Wellcome Trust Centre for Neuroimaging, which is funded by the Wellcome Trust.*